

X-ray-absorption spectroscopy of CoSi_2

W. F. Pong and Y. K. Chang

Department of Physics, Tamkang University, Tamsui, Taiwan 251, Republic of China

R. A. Mayanovic

Department of Physics and Astronomy, Southwest Missouri State University, Springfield, Missouri 65804

G. H. Ho and H. J. Lin

Synchrotron Radiation Research Center (SRRC), Hsinchu, Taiwan 300, Republic of China

S. H. Ko*

Department of Materials Engineering, Rensselaer Polytechnic Institute, Troy, New York 12180

P. K. Tseng

Department of Physics, Tamkang University, Tamsui, Taiwan 251, Republic of China

C. T. Chen[†]

AT&T Bell Laboratories, Murray Hill, New Jersey 07974

A. Hiraya[‡]

Institute for Molecular Science, Myodaiji, Okazaki 444, Japan

M. Watanabe

Research Institute for Scientific Measurements, Tohoku University, Aoba, Sendai 980, Japan

(Received 9 June 1995)

X-ray-absorption near-edge structure (XANES) spectra of thin-film CoSi_2 were measured at the Si K edge and Co L_3 edge using the total electron yield mode. The Si K -edge results for CoSi_2 showed a dramatic reduction of intensity in the first broad feature accompanied by a rise in a relatively strong and sharp feature at higher binding energies when compared to XANES spectra for crystalline Si. We attribute these two features to the Si $1s$ photoelectron excitations to a broad Si $3p$ nonbonding band and a relatively narrow band of hybridized Si p -Co $3d$ antibonding states, respectively. Analysis of the Co L_3 -edge white line spectra for CoSi_2 reveals the appearance of a triple structure, which can be attributed to excitations to the unoccupied Co $3d$ nonbonding states and hybridized antibonding Co ($3d,4s$)-Si p states. [S0163-1829(96)04924-7]

I. INTRODUCTION

The electronic properties of thin-film transition-metal (TM) silicides such as CoSi_2 have attracted great attention over the last decade because of their potential for widespread applications in electronic devices. A detailed understanding of the electronic structure of this material is important for technological applications. The electronic structure of CoSi_2 has been studied theoretically by several investigators using band-structure calculations.¹⁻⁴ Their calculations indicate that Si p -TM d hybridization contributes substantially to the density of states (DOS) near the Fermi level. Photoemission spectroscopy^{5,6} and soft-x-ray emission^{7,8} which give useful information regarding the valence-band DOS of solids, are in good agreement with calculated band structures concerning the nature of Si p -TM d hybridization as well as Si s -TM d bonding at or near the valence-band edge in TM silicides. X-ray-absorption near-edge structure (XANES) can provide complementary information concerning unoccupied states just above the Fermi level. Several Si K -edge^{4,9} and Co L_3 -edge^{4,10} XANES investigations of bulk CoSi_2 have

been reported recently. In this paper we present an analysis of Si K -edge and Co L_3 -edge XANES spectra of thin-film CoSi_2 grown by a thermal reaction process. The major goal is to gain a deeper understanding of the chemical bonding in thin-film CoSi_2 . We discuss the results of XANES spectra of thin-film CoSi_2 and compare our findings with other experimental data and theoretical calculations of DOS from earlier studies.

II. EXPERIMENT

Thin-film CoSi_2 was grown by rapid thermal annealing of Co sputtered on a crystalline Si(100) substrate. Thin-film Si/Co was first annealed at 500 °C for 60 sec, leading to compound formation of coexisting $\text{CoSi}/\text{Co}_2\text{Si}$, and then again at 675 °C for 60 sec, forming the metallic CoSi_2 phase with a thickness of $\cong 2560$ Å. The reaction path of the top layer appears to have proceeded in the following manner: $\text{Co} \rightarrow \text{Co}_2\text{Si} \rightarrow \text{CoSi} \rightarrow \text{CoSi}_2$. Details of the preparation procedure have been described elsewhere.¹¹ In addition, a sample of Si/Co was prepared by depositing Co (thickness ≤ 100 Å)

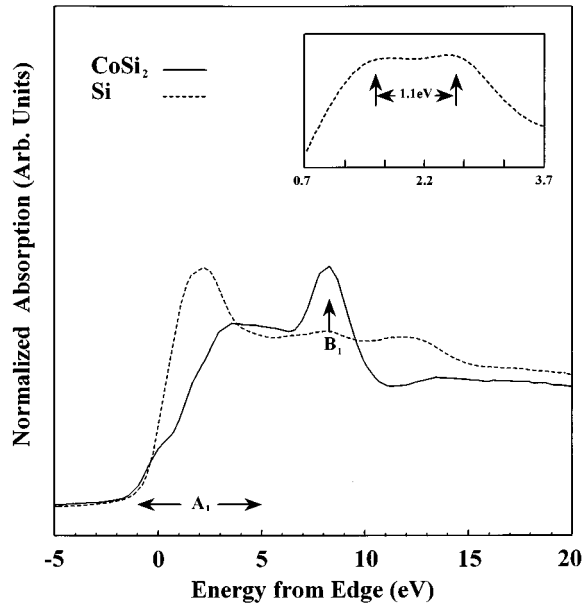


FIG. 1. Normalized Si K near-edge absorption spectra. The threshold region of crystalline Si is inset on a magnified scale.

onto a Si(100) substrate. The metal concentration profile and homogeneity of CoSi_2 were verified by Rutherford backscattering spectrometry and electron-probe microanalysis, and its structure was characterized by x-ray diffraction. The results from this analysis, along with the O K -edge XANES (Ref. 12) and Co K -edge extended x-ray absorption fine-structure (EXAFS) measurements presented below, show negligible oxidation of CoSi_2 .

Si K -edge x-ray-absorption spectra of thin-film Si/ CoSi_2 and crystalline Si(100) were obtained at beamline 1A at the Ultraviolet Synchrotron Orbital Radiation Facility (UVSOR), Institute for Molecular Science, Okazaki, Japan. The spectra were measured in the total electron yield (TEY) mode with an electron multiplier, using a double-crystal InSb(111) monochromator. Photon energies were calibrated using the M_5 edge of a Au photocathode. Co L_3 -edge XANES of Si/ CoSi_2 and Si/Co were measured using the AT&T Bell Laboratories Dragon beamline at the National Synchrotron Light Source (NSLS), Brookhaven National Laboratory. XANES spectra were obtained in the TEY mode with a channeltron detector, using the 1200-1/mm grating of the monochromator. The energy scale was calibrated using the well-known spectrum of a CaF_2 thin film. The energy resolution was set at ~ 1.0 eV in the Si K edge for InSb(111) and ~ 0.4 eV in the Co L_3 edge for the grating monochromator, respectively. All measurements were made at room temperature.

III. RESULTS AND DISCUSSION

Figures 1 and 2 show the Si K -edge XANES spectra for Si/ CoSi_2 and crystalline Si(100), and the Co L_3 -edge white line spectra of Si/ CoSi_2 and Si/Co. After pre-edge background subtraction, the spectra were normalized using the incident beam intensity I_0 and scaled to the maximum of the peak heights. Due to the surface sensitivity of TEY measurements, we believe that the spectra in Figs. 1 and 2 predomi-

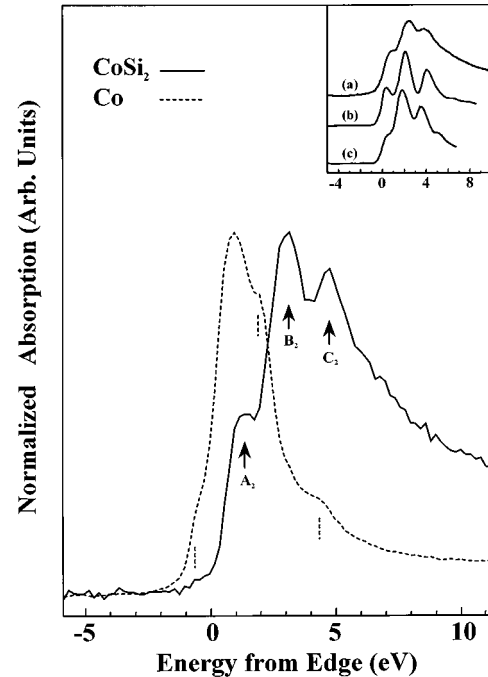


FIG. 2. Normalized Co L_3 near-edge absorption spectra. The inset represents the experimental absorption spectrum (a) and the convolution of theoretical DOS with a Gaussian broadening [(b) and (c)] of CoSi_2 (from Ref. 10).

nantly reflect the electronic and local structure environments of the outermost layers (on the order of 100 Å) of CoSi_2 (in Si/ CoSi_2), Co (in Si/Co), and Si [in crystalline Si(100)], respectively. For x-ray energies in the XANES region, the excited photoelectron undergoes transition from a core state to an unoccupied state; the final state is determined in relation to the initial state by the dipole selection rule. Zero energy for the Si K edge (1839.3 eV) XANES spectra in Fig. 1 was selected at the inflection point of the threshold in crystalline Si. In the case of crystalline Si, the characteristic double-peak feature near 1.5 and 2.6 eV above the edge and its approximate 1.1-eV energy separation were observed. Although calculated partial density of states for p symmetry is unavailable, Woicik *et al.* assigned this double peak to the Si $1s$ to first two Si p unoccupied conduction-band states.¹³ This splitting of the Si K -edge XANES spectrum for crystalline Si is also in agreement with earlier published studies.^{14,15} Hitchcock *et al.*¹⁵ interpreted the two peaks as the Si $1s$ to unoccupied Si $3p$ conduction-band excitations, based on the idea of crystal symmetry.

As shown in Fig. 1, the feature A_1 (occurring between -1 and 5 eV) found in the spectrum of CoSi_2 is significantly broader than in the Si XANES spectrum and contains some weak structures at the threshold jump region. Its intensity above the edge is also reduced dramatically, while the main inflection point shifts toward higher energies with respect to crystalline Si. In addition, feature B_1 located near 8.2 eV above the Si K edge is significantly enhanced for CoSi_2 compared to the spectrum for crystalline Si. In comparing our Si K -edge spectrum for CoSi_2 to those previously reported,^{4,9} we notice a discrepancy in feature B_1 . Our data reveal a much stronger and sharper B_1 feature than that presented by Lerch *et al.*⁴ and Weijs *et al.*⁹ Their spectra for

CoSi₂ showed that the energy dependence in the region between -1 and 4 eV was similar to that observed for our data, with a lower relative intensity. However, contrary to our data, their results displayed a long plateau between 4 and 12 eV above the edge, which slowly decreased as a function of energy. In addition, the spectrum of Lerch *et al.* also exhibited additional weak oscillating structure in the plateau region. We have no conclusive explanation for these differences.

As mentioned above, the threshold in the Si *K*-edge XANES spectrum of CoSi₂ is shifted toward higher binding energies with respect to the spectrum of crystalline Si. This reflects the fact that the chemical state of the absorbing Si atoms is changed in CoSi₂, as exhibited in the details of the electronic structure of the valence bands, relative to its state in the crystalline Si. As is well known, silicon has the diamond cubic structure in which strong mutual interaction between the sp^3 orbitals results in the formation of tetrahedrally coordinated sp^3 hybrid bonds. Conversely, Si-Co bonding in CoSi₂ is much less covalent and substantially more metallic in nature. It is therefore not surprising that the electronic properties as well as the local structure surrounding the Si atom are quite different between CoSi₂ and crystalline Si. Experimental evidence derived from systematic photoemission studies performed by Franciosi *et al.*⁶ indicates that the binding energies of silicides shift with different stoichiometries. Core-hole effects⁹ and charge transfer effects^{2,16} may also influence the energy shift of the threshold feature in CoSi₂, although there still exists some controversy concerning the effects of charge transfer between Si and metal in TM silicides.^{1,17} Provided that features A_1 and B_1 are related to the bonding states, then their interpretation in terms of Si *p* orbitals and hybridized Si *p* and Co *3d* orbitals contributing to the DOS of CoSi₂ follows accordingly.

Now let us turn to the Co *L*₃-edge x-ray-absorption spectra for thin-film CoSi₂ and Co. Shown in Fig. 2, the white line peaks at the Co *L*₃ edge are attributed to the excitation of electrons from Co $2p_{3/2}$ core states to final unoccupied Co *3d* states above the Fermi level. Zero energy for the Co *L*₃ edge (778.7 eV) was selected at the central point of the jumping threshold in Co. In general, the *L*₃ white line peak position and shape for Si/Co are in agreement with the absorption spectrum of Co grown on Cu(100).¹⁸ However, there are several satellite structures observed in our data, indicated in Fig. 2 by vertical dotted lines near -0.6 , 2.0 , and 4.4 eV. It is likely that these satellite structures reveal the chemical states of the interfacial Co atoms at the Co-Si substrate interface, for which there may be two contributions. One source may be the interdiffusion of Co into Si at very low coverage producing a region of different stoichiometry.¹⁹ A second source may be the formation of interface states²⁰ for Co atoms located close to the interface between the Co layer and the Si surface. We suspect these satellite structures may also be associated with partial oxidation of the top Co layer,¹² which was primarily caused by leaving the sample surface open to atmosphere.

It is quite obvious from Fig. 2 that the Co *L*₃-edge white line region of the CoSi₂ spectrum is different from that of Co, as its main features clearly display three structures, marked in the figure as A_2 , B_2 , and C_2 (located near 1.4 ,

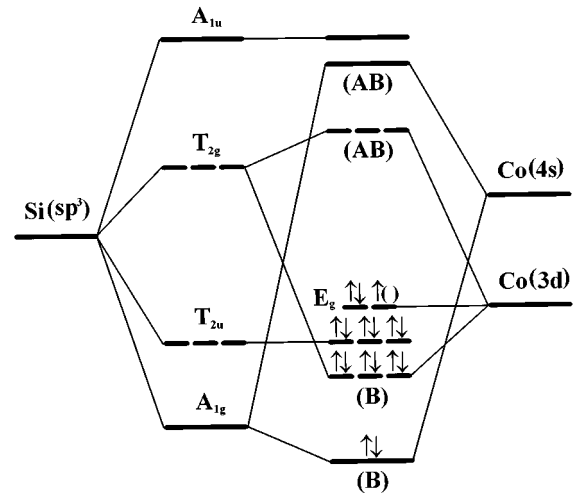


FIG. 3. Schematic energy diagram showing respective atomic levels forming Co *3d,4s* and Si sp^3 bands of CoSi₂. The labels A_{1g} , T_{2u} , E_g , etc. indicated the irreducible representations of the cubic point group. AB and B denote antibonding and bonding states, respectively. \uparrow and \downarrow denote states for spin up and spin down, respectively (not to scale).

3.2 , and 4.8 eV, respectively), as opposed to a single peak in the case of Co. Furthermore, feature A_2 in CoSi₂ has an approximate 0.4 -eV energy shift to higher energies relative to the main peak of thin-film Co. We infer, as for the Si *K*-edge shift, that the shift in the main region of the Co *L*₃-edge XANES of CoSi₂ is primarily due to the effect of change in the electronic configuration of the absorbing atom (Co). We note that the CoSi₂ spectrum presented here not only shows better resolution, but is also in good agreement with the experimental data and the theoretical DOS obtained by Eisebitt *et al.*¹⁰ The theoretical DOS was calculated by Tersoff and Hamann¹ and by van Leuken.²¹ A convolution of the two theoretical DOS with the instrumental and core-hole lifetime broadening leads to better agreement with our experimental results (see inset of Fig. 2), regarding features A_2 , B_2 , and C_2 of the Co *L*₃-edge spectrum. (In spite of encouraging agreement, there was still a slight shift of the relative energy position of the triple structures in comparison between theoretical and experimental data.) We infer that features A_2 , B_2 , and C_2 of the Co *L*₃-edge spectrum are directly related to hybridization between the Co *3d,4s* and Si sp^3 orbitals. This can be explained with greater clarity using Fig. 3, which shows a schematic representation of the Co *3d*, Co *4s*, and Si sp^3 bands of CoSi₂ derived from their respective atomic levels. Our model most closely resembles a model derived from electronic structure calculations for “bulklike” CoSi₂ by van den Hoek, Ravenek, and Baerends.²² In this model, the Si sp^3 states become hybridized with Co *3d* and Co *4s* orbitals in CoSi₂, resulting in a band structure having two nonbonding E_g (Co *3d*) and T_{2u} (Si *p*) states, as well as hybridized Co *3d*-Si *p* and Co *4s*-Si *s* states, which are represented by T_{2g} and A_{1g} , respectively.

It is important to stress that an understanding of the “bulklike” characteristics (i.e., Young’s modulus, electrical conductivity, etc.) requires knowledge of the local atomic structure of the thin-film CoSi₂. In a separate study, total

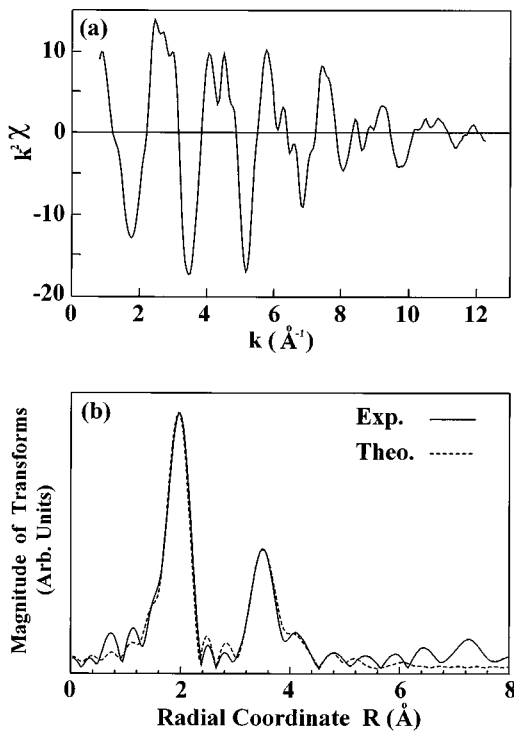


FIG. 4. (a) Normalized Co K -edge EXAFS oscillations $\chi(k)$ weighted by k^2 for CoSi₂. (b) Magnitude of Fourier transform of the EXAFS $k^3\chi$ data from $k=3.4$ to 12 \AA^{-1} . Structural parameters of two nearest neighbors obtained by fitting the Co K -edge EXAFS spectrum: $N_{\text{Co-Si}}=8$, $R_{\text{Co-Si}}=2.32 \pm 0.01 \text{ \AA}$, $\sigma_{\text{Co-Si}}^2=(5.10 \pm 0.07) \times 10^{-3} \text{ \AA}^2$, $N_{\text{Co-Co}}=12$, $R_{\text{Co-Co}}=3.80 \pm 0.02 \text{ \AA}$, $\sigma_{\text{Co-Co}}^2=(8.14 \pm 0.03) \times 10^{-3} \text{ \AA}^2$. N is the coordination number, R the nearest-neighbor distance, and σ^2 the mean-square vibrational amplitude.

electron yield EXAFS measurements²³ were performed at the Co K edge on our thin-film CoSi₂. The normalized EXAFS oscillation $\chi(k)$ weighted by k^2 for Co K edge and the corresponding Fourier transforms of the $k^3\chi$ data are shown in Fig. 4.²⁴ Further analysis involved use of the combination of the multiple-scattering EXAFS computer program FEFF5 (Ref. 25) and the nonlinear least-squares fitting computer program FEFFIT.²⁶ As shown, the quality of the fit in Fig. 4 is quite good. Structure results from fitting indicate that the absorbing central Co atom is surrounded by eight nearest-neighbor Si atoms at $2.32 \pm 0.01 \text{ \AA}$ and twelve next-nearest-neighbor Co atoms at $3.80 \pm 0.02 \text{ \AA}$, which is consistent with CoSi₂ having the fluorite structure. Our thin-film sample is indeed similar to that of “bulklike” CoSi₂ reported in the literature.²⁷ This justifies the use of the electronic structure model, which is very similar to the one developed by van den Hoek, Ravenek, and Baerends, to explain the XANES of thin-film CoSi₂.

We now discuss the XANES spectra of CoSi₂ in detail in relation to the electronic structure model shown in Fig. 3. Referring to Fig. 3, we can see that all the antibonding states are empty, but the bonding and the nonbonding states are filled except for a vacancy for one electron (indicated by empty brackets) in the nonbonding E_g states. Subsequently, our assignments for features A_2 , B_2 , and C_2 of the CoSi₂ spectrum in Fig. 2 can be made more specific. Since the

photoelectrons originating from p states become excited to the first unoccupied d -like and s -like states above the Fermi level, the most reasonable conclusion is that features A_2 and B_2 correspond to $2p_{3/2}$ electrons making transitions to both partially unoccupied nonbonding E_g states and empty antibonding T_{2g} states. A similar assignment for features A_2 and B_2 in the Co L_3 -edge white line region of the CoSi₂ spectrum was given by Eisebitt *et al.*¹⁰ The E_g states have mainly Co $3d$ character, constitute metallic bonds, and have characteristics similar to pure Co metal. These states are located in energy between the bonding and antibonding states. The antibonding T_{2g} states are formed from hybridized Co $3d$ -Si p states, for which the degree of hybridization is determined by the extent of Co $3d$ and Si p orbital wave-function overlap, which in turn is reflected in the DOS. The crystal-field splitting of the T_{2g} and E_g states is 1.8 eV, which is well characterized by Tersoff and Hamann in terms of a *quasigap* in the density of states near the Fermi level separating bonding and antibonding states. In addition, feature C_2 can be assigned to the Co $2p_{3/2} \rightarrow$ antibonding A_{1g} transition. The antibonding A_{1g} states are derived from Co $4s$ orbitals interacting with Si s orbitals.

The Si K -edge spectrum for thin-film CoSi₂ can be satisfactorily interpreted using the energy-level diagram in Fig. 3. The main feature of the Si K -edge XANES spectrum for bulk CoSi₂ was previously attributed to the unoccupied antibonding Si p states.⁹ More specifically, referring to Fig. 3, we infer that feature B_1 of our Si K -edge XANES spectrum for thin-film CoSi₂ can be attributed mainly to Si $1s \rightarrow$ antibonding T_{2g} transitions. Since feature B_1 is relatively narrow, the antibonding T_{2g} band has a relatively narrow energy width. If feature B_1 is attributed to transitions to the antibonding T_{2g} states, then the question arises of how to ascribe feature A_1 in terms of the chemical bonding in DOS. The nonbonding T_{2u} states have Si p symmetry and theoretically have the highest probability to be considered as the states in connection with feature A_1 . However, we do not expect to see any peaks in the Si K -edge XANES spectrum provided that the nonbonding T_{2u} states are completely filled (see Fig. 3).

Regarding feature A_1 in Fig. 1, we see clearly that the threshold of the XANES for CoSi₂ is at the same energy as for crystalline Si. This implies that feature A_1 is associated with unoccupied Si $3p$ states, in agreement with the conclusions of Hitchcock *et al.*¹⁵ In fact, linear augmented-plane-wave band-structure calculations for NiSi₂ (Ref. 5) suggest that the Si $3p$ free-electron-like band, which is principally responsible for the metallic character of the material, is spread over a wide energy range in comparison with the Ni $3d$ band, which has a relatively narrow energy width in NiSi₂. Furthermore, it has been observed previously that in free-electron-like metallic systems, one obtains additional weak structures at the threshold of XANES as the result of valence electron excitations induced by the electron gas-core hole interactions.²⁸ Therefore, we conclude that feature A_1 is due to Si $1s \rightarrow$ nonbonding T_{2u} (Si $3p$) transitions.

Such states are available for photoabsorption transitions because the Si $3p$ free-electron-like band has strong DOS contributions extending up to the Fermi level, causing electron transfer from the Si $3p$ orbitals to the Co “atomic”

states. This causes the nonbonding T_{2u} states to be partially unoccupied above the Fermi level and thus gives rise to a smooth and broad feature extending ~ 5 eV above the edge in the spectrum. The nature of electron charge transfer from Si to metal atom sites in TM silicides has been discussed previously by Lambrecht and co-workers.^{2,16}

The considerably weaker intensity and broadness of feature A_1 in comparison to B_1 can be attributed to a small number of unoccupied states in the broad low-lying nonbonding T_{2u} band and a relatively larger number of unoccupied states in the antibonding T_{2g} band. On the whole, the former shows that the Si $3p$ -symmetry final density of states is small and spreads over a wide energy range. Meanwhile, the latter reflects the increasing Co $3d$ density of states above the Fermi level, in agreement with the natural characteristics of $3d$ symmetric states, giving rise to the narrow energy width. Finally, we would like to point out that due to charge transfer effects, the unoccupied nonbonding T_{2u} band is situated above the Fermi level. As a consequence, we locate the Fermi level in the region between the nonbonding T_{2u} states and the bonding T_{2g} states, whereas van den Hoek, Ravenek, and Baerends²² suggested that the Fermi level was mainly in the region of nonbonding E_g and T_{2u} states.

IV. CONCLUSION

In summary, our analysis of the XANES spectra indicates significant effects due to photoelectron excitations to Si p -

and Co ($3d,4s$)-derived orbitals in thin-film CoSi_2 . Three distinct peaks appear in the Co L_3 -edge white line region, which are attributed to photoelectron transitions to the nonbonding Co $3d$ states and hybridized Co ($3d,4s$)-Si p antibonding states. We find very good agreement between Co L_3 -edge XANES spectra measured on our thin-film CoSi_2 and ones measured previously on ion-beam-synthesized CoSi_2 . In the Si K -edge XANES spectrum of CoSi_2 , a relatively narrow feature B_1 is associated with photoelectron excitations to hybridized Si p -Co $3d$ antibonding states. Feature B_1 is significantly more pronounced and sharper in our Si K -edge XANES spectrum for thin-film CoSi_2 in comparison to the same measured previously from bulk CoSi_2 . Finally, we speculate that the threshold region feature A_1 of the same spectrum is due to transitions to the nonbonding T_{2u} (Si $3p$) states which are partially unoccupied due to charge transfer from Si to Co in CoSi_2 .

ACKNOWLEDGMENTS

One of the authors (W.F.P.) acknowledges support by the National Science Council of the R.O.C., under Contract No. NSC84-2112-M-032-010. This work was performed on beamline 1A at UVSOR, the Institute for Molecular Science (IMS), and AT&T Bell Laboratories Dragon beamline at NSLS.

*Present address: Applied Materials, Santa Clara, California 95054.

[†]Present address: Synchrotron Radiation Research Center (SRRC), Hsinchu, Taiwan 300, Republic of China.

[‡]Present address: Department of Material Science, Hiroshima University, Hiroshima 739, Japan.

¹J. Tersoff and D. R. Hamann, Phys. Rev. B **28**, 1168 (1983).

²W. R. L. Lambrecht, N. E. Christensen, and P. Blöchl, Phys. Rev. B **36**, 2493 (1987).

³L. F. Mattheiss and D. R. Hamann, Phys. Rev. B **37**, 10 623 (1988).

⁴P. Lerch, T. Jarlborg, V. Codazzi, G. Loupiaz, and A. M. Flank, Phys. Rev. B **45**, 11 481 (1992).

⁵Y. J. Chabal, D. R. Hamann, J. E. Rowe, and M. Schlüter, Phys. Rev. B **25**, 7598 (1982).

⁶A. Franciosi, J. H. Weaver, and F. A. Schmidt, Phys. Rev. B **26**, 546 (1982).

⁷H. Nakamura, M. Iwami, M. Hirai, M. Kusaka, F. Akao, and H. Watabe, Phys. Rev. B **41**, 12 092 (1990).

⁸J. J. Jia, T. A. Callcott, W. L. O'Brien, Q. Y. Dong, J. E. Rubensson, D. R. Mueller, D. L. Ederer, and J. E. Rowe, Phys. Rev. B **43**, 4863 (1991); J. J. Jia, T. A. Callcott, W. L. O'Brien, Q. Y. Dong, D. R. Mueller, D. L. Ederer, Z. Tan, and J. I. Budnick, *ibid.* **46**, 9446 (1992).

⁹P. J. W. Weijs, M. T. Czyzyk, J. F. van Acker, W. Speier, J. B. Goedkoop, H. van Leuken, H. J. M. Hendrix, R. A. de Groot, G. van der Laan, K. H. J. Buschow, W. Wiech, and J. C. Fuggle, Phys. Rev. B **41**, 11 899 (1990).

¹⁰S. Eisebitt, T. Böske, J. E. Rubensson, J. Kojnok, W. Eberhardt, R. Jevasinski, S. Mantl, P. Skytt, J. H. Guo, N. Wassdahl, J. Nordgren, and K. Hollmack, Phys. Rev. B **48**, 5042 (1993).

¹¹S. H. Ko, S. P. Murarka, and A. R. Sitaram, J. Appl. Phys. **71**, 5892 (1992).

¹²We have recently measured the O K -edge XANES spectra of CoSi_2 , Si, and Co. The spectra of CoSi_2 and Si are similar to that of pure molecular oxygen [see M. W. Ruckman *et al.*, Phys. Rev. Lett. **67**, 2533 (1991)] suggesting predominantly O-O bonding of molecular oxygen on the surfaces of the samples. Together with the Co K -edge EXAFS results shown below, these characterization studies show negligible oxidation of CoSi_2 . On the other hand, the O K -edge XANES spectrum of Co shows O-Co bonding may have occurred in that sample.

¹³J. C. Woicik, B. B. Pate, and P. Pianetta, Phys. Rev. B **39**, 8593 (1989); J. C. Woicik and P. Pianetta, in *Synchrotron Radiation Research: Advances in Surface and Interface Science, Vol. 2, Issues and Technology*, edited by R. Z. Bachrach (Plenum, New York, 1992).

¹⁴N. Nagashima, A. Nakano, K. Ogata, M. Tamura, K. Sugawara, and K. Hayakawa, Phys. Rev. B **48**, 18 257 (1993).

¹⁵A. P. Hitchcock, T. Tyliczszak, P. Aebi, J. Z. Xiong, T. K. Sham, K. M. Baines, K. A. Mueller, X. H. Feng, J. M. Chen, B. X. Yang, Z. H. Lu, J. M. Baribeau, and T. E. Jackman, Surf. Sci. **291**, 349 (1993); A. P. Hitchcock, T. Tyliczszak, P. Aebi, X. H. Feng, Z. H. Lu, J. M. Baribeau, and T. E. Jackman, *ibid.* **301**, 260 (1994).

¹⁶W. R. L. Lambrecht, Phys. Rev. B **34**, 7421 (1986). (The assumption of the core-level shifts is based on the charge transfer from Si toward Ni in NiSi_2 . One may expect similar quality of the description of the CoSi_2 , since CoSi_2 and NiSi_2 have some fluorite structures as CaF_2 .)

¹⁷O. Bisi, L. W. Chiao, and K. N. Tu, Phys. Rev. B **30**, 4664 (1984).

- ¹⁸T. Böske, W. Clemens, C. Carbone, and W. Eberhardt, *Phys. Rev. B* **49**, 4003 (1994).
- ¹⁹G. W. Rubloff, *Surf. Sci.* **132**, 268 (1983).
- ²⁰G. Rossi, X. Jin, A. Santaniello, P. Depadova, and D. Chandesris, *Phys. Rev. Lett.* **62**, 191 (1989).
- ²¹H. van Leuken, Ph.D. thesis, Katholieke Universiteit Nijmegen, 1986.
- ²²P. J. van den Hoek, W. Ravenek, and E. J. Baerends, *Phys. Rev. Lett.* **25**, 1743 (1988).
- ²³K. Kemmer, Z. Wang, R. A. Mayanovic, and B. A. Bunker, *Nucl. Instrum. Methods Phys. Res.* **71**, 345 (1992).
- ²⁴W. F. Pong *et al.* (unpublished).
- ²⁵J. M. de Leon, Y. Yacoby, E. A. Stern, and J. J. Rehr, *Phys. Rev. B* **42**, 10 843 (1990); J. J. Rehr, J. M. de Leon, S. I. Zabinsky, and R. C. Albers, *J. Am. Chem. Soc.* **113**, 5135 (1991).
- ²⁶A. I. Frenkel, E. A. Stern, M. Qian, and M. Newville, *Phys. Rev. B* **48**, 12 449 (1993).
- ²⁷G. Rossi, X. Jin, A. Santaniello, P. Depadova, and D. Chandesris, *Phys. Rev. Lett.* **62**, 191 (1989); Z. Tan, J. I. Budnick, F. H. Sanchez, G. Torrillon, F. Namavar, and H. C. Hayden, *Phys. Rev. B* **40**, 6368 (1989); Z. Tan, F. Namavar, S. M. Heald, C. E. Bouldin, and J. C. Woicik, *ibid.* **46**, 4077 (1992); S. Eisebitt, J. E. Rubensson, T. Böske, and W. Eberhardt, *ibid.* **48**, 17 388 (1993).
- ²⁸E. Zaremba and K. Sturm, *Phys. Rev. Lett.* **66**, 2144 (1991).